Mem. S.A.It. Vol. 80, 870

**Memorie** della

# Observational determinations of the proton to electron mass ratio in the early Universe

R. Thompson

University of Arizona – Steward Observatory, Tucson, Arizona 85721, USA
e-mail: rit@email.arizona.edu

**Abstract.** The values of the fundamental physical constants determine the nature of our universe from the height of mountains on earth to the evolution of the universe over its history. One of these constants is $\mu = M_P/M_e$ the ratio of the proton to electron mass. Astronomical observations provide a determination of this ratio in the early universe through observations of molecular absorption and emission lines in distant objects. Observations of molecular hydrogen in distant damped Lyman Alpha clouds provide a measurement of $\mu$ at a time when the universe was only 20% of its present age. To date there is no evidence for a change in $\mu$ at the level of 1 part in $10^5$. This limit produces an observational constraint on quintessence theories for the evolution of the universe and Super Symmetric theories of elementary particles.

**Key words.** Cosmology: observations

## 1. Introduction

Speculation on the time stability of the fundamental constants extends back at least to the middle of the previous century when Dirac (1937), Teller (1948) and Gamow (1967) first discussed the possibility of time variation of the fundamental constants. Observational constraints on the time variation of fundamental constants has centered primarily on the fine structure constant $\alpha$ and the ratio of the proton to electron mass $\mu$. This review concentrates on observational constraints on $\mu$, therefore we will only discuss $\alpha$ in context with variations in $\mu$. It was first pointed out by Thompson (1975) that observations of the absorption lines of molecular hydrogen in distant damped Lyman $\alpha$ (DLA) clouds provided an opportunity to measure $\mu$ in the early universe. Many of the early observations are discussed in Thompson et al. (2009). The most recent observations are given by Reinhold et al. (2006), Ubachs et al. (2007), Wendt and Reimers (2008), King et al. (2009) and Thompson et al. (2009). Although the first of these studies, Reinhold et al. (2006) and Ubachs et al. (2007) indicated a possible change in the value of $\mu$ the subsequent studies found no change in $\mu$ at the $10^{-5}$ level using the same data. In our galaxy and the more local universe radio observations of the inversion lines of ammonia have been used to measure the value of $\mu$ and to look for spatial variations in its value. The galaxy B0218+357 at a redshift of 0.6847 has been detected in ammonia and a limit on $\Delta\mu/\mu$ of $\Delta\mu/\mu \leq 1.8 \times 10^{-7}$ has been established (Flambaum & Kozlov

*Send offprint requests to*: R. Thompson

(2007) and Murphy et al. (2008)). Milky Way measurements of ammonia spectra by Levshakov, Molaro & Kozlov (2008) have been cited as evidence for possible spatial variations of $\mu$ as predicted by some dark energy theories. These observations are awaiting further confirmation. For the rest of this review we will concentrate on the early universe $\mu$ observations.

## 2. Molecular sensitivity to $\mu$

As pointed out in Thompson (1975) to first order the rotational energy levels of molecules are directly proportional to $\mu$ through the moment of inertia and the vibrational energy levels are proportional to $\sqrt{\mu}$ as in a harmonic oscillator. This sensitivity to $\mu$ means that transitions from the ground states to upper electrical, vibrational and rotational states have unique shifts in wavelength for a given change in $\mu$. A schematic of these transitions is given in Figure 1.

Although implicit in earlier work Varshalovich & Levshakov (1993) were the first to formally introduce the sensitivity factor $K_i$ for each line i which is defined as

$$K_i = \frac{d \ln \lambda_i}{d \ln \mu} = \frac{\mu}{\lambda_i}\frac{d\lambda_i}{d\mu} = -\frac{\mu}{\nu_i}\frac{d\nu_i}{d\mu} \tag{1}$$

With this definition the observed wavelength $\lambda_i$ is related to the rest wavelength $\lambda_0$ by

$$\lambda_i/\lambda_0 = (1+z)(1+K_i\Delta\mu/\mu) \tag{2}$$

Traditionally data analysis has been carried out by linear fitting of the reduced redshift $\zeta$ of each line versus the sensitivity factor $K_i$ for the lines. The reduced redshift $\zeta$ is defined by

$$\zeta = \frac{z_i - z_Q}{1 + z_Q} = \Delta\mu/\mu K_i \tag{3}$$

where $z_i$ is the measured redshift of the individual lines and $z_Q$ is the intrinsic redshift of the DLA system containing the $H_2$ lines. Figure 2 gives an example of such a plot taken from Thompson et al. (2009). Note that the fitted slope in this type of plot is $\Delta\mu/\mu$. Also notice that the reduced redshift axis is multiplied by $10^6$.

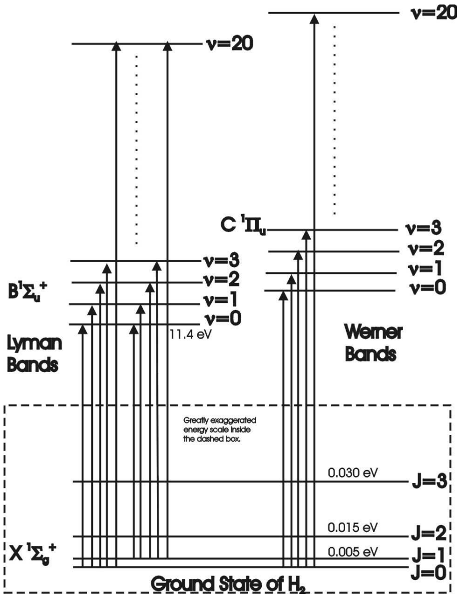


**Fig. 1.** This figure depicts some of the allowed transitions of molecular hydrogen for the Lyman and Werner series of electronic transitions. Although changes in the rotational quantum number are limited to $0, \pm 1$ the change in the vibrational quantum number is unrestricted. In general the higher the vibrational quantum number of the upper state the higher the sensitivity to a change in $\mu$. Note that the scale of the lower state rotational energy levels is greatly exaggerated relative to the upper states.

## 3. $H_2$ difficulties and advantages

The measurement of $\mu$ through $H_2$ absorption lines in DLAs has both difficulties and advantages. A primary difficulty is that very few DLAs have measurable amounts of $H_2$. In fact there are only about a dozen known systems, however, some of the presentations in this JD have indicated that more may be available in the near future. A second major difficulty is that the Lyman and Werner lines lie in the Lyman $\alpha$ forest where most of them are contaminated by other lines. It is quite hard to find lines that are clear of significant contamination. Finally the sensitivity factors are low, on the order of $10^{-2}$, since the primary shift is in the vibrational energy levels which are about $10^{-2}$ of the electronic energy which is basically unshifted. There are also several ad-

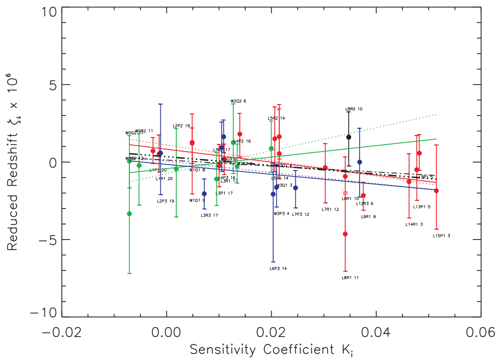


**Fig. 2.** The reduced redshift versus sensitivity factor plot for Q0347-383. The symbols are color coded according to the rotational level of the lower electronic state. J=0(black), J= 1(red), J=2(green), J=3(blue). The solid line is the weighted fit and the dotted line is the unweighted fit to the individual J levels. The thick dash 3 dot line is the weighted fit and the thick dash dot line the unweighted fit to all J levels combined. The transitions are labeled with the last number being the order. The orders are the observed order with the true order being 126 minus the printed number.

vantages of using $H_2$ measurement to determine the value of $\mu$. There are several hundred available $H_2$ lines, therefore many lines with the same ground state can be measured to eliminate different kinematics between regions of different excitation temperatures as an error source. There are also very accurate measurement of the rest wavelengths of the observed lines. Current accuracies are a few parts in $10^8$ (Ubachs et al. 2007). However, since the sensitivity factors are in the range of $10^{-2}$, pushing past an accuracy in $\mu$ of better than $10^{-6}$ will require improved laboratory measurements. A further advantage is that lines with greatly differing sensitivities are in close vicinity in wavelength. This is due to the overlap between the Lyman and Werner bands. These combinations greatly reduce errors due to wavelength calibration. The small number of sources with measurable $H_2$ systems means that only a few sources have $H_2$ $\mu$ measurements. Table 1 shows the published measurements to date.

**Table 1.** Sources with measured values of $\mu$

| Source | Redshift | References |
|---|---|---|
| Q0528-250 | 2.811 | a,b,c,d |
| Q1232+082 | 2.338 | e |
| Q0347-383 | 3.025 | d,e,f,g,h,i,j,k,l,m,n |
| Q0405-443 | 2.595 | d,e,f,g,h,i,j,k,l,m,n |
| Q1331+170 | 1.776 | o |

a) Foltz, Chaffee & Black (1988) b) Cowie & Songaila (1995) c) Potekhin et al. (1998) d) King et al. (2009) e) Ivanchik et al. (2002) f) D'Odorico et al. (2001) g) Ivanchik et al. (2003) h) Ivanchik et al. (2005) i) Levshakov et al. (2002) j) Ubachs & Reinhold (2004) k) Reinhold et al. (2006) l) Ubachs et al. (2007) m) Wendt and Reimers (2008) n) Thompson et al. (2009)

## 4. Current state of $\Delta\mu/\mu$ measurements

To date the only claim for a detection of a non-zero $\Delta\mu/\mu$ has been Reinhold et al. (2006) and the subsequent follow up on the same data by Ubachs et al. (2007). These two works claimed a positive detection with $\Delta\mu/\mu = (2.45\pm0.49)\times 10^{-5}$ for Q0347-383 and Q0405-443 utilizing VLT UVES data obtained in 2002 and 2003. Subsequent reanalysis of the same data by King et al. (2009), Wendt and Reimers (2008) and Thompson et al. (2009) failed to confirm this detection and have largely attributed the erroneous result to errors in the wavelength calibration of the UVES pipeline during that epoch which have subsequently been rectified. King et al. (2009) included an extra UVES data set for Q0528-250 to improve their limit to $\Delta\mu/\mu = (2.6 \pm 3.0) \times 10^{-6}$ for the combination of the 3 observations. Figure 3 shows the combined Q0347-383 and Q0405-443 data in a reduced redshift versus sensitivity factor plot from Thompson et al. (2009)

## 5. Systematic errors

An understanding of the sources of systematic error are extremely important for precision measurements. In the following section we review some of the possible systematic errors that could affect $\mu$ measurements.

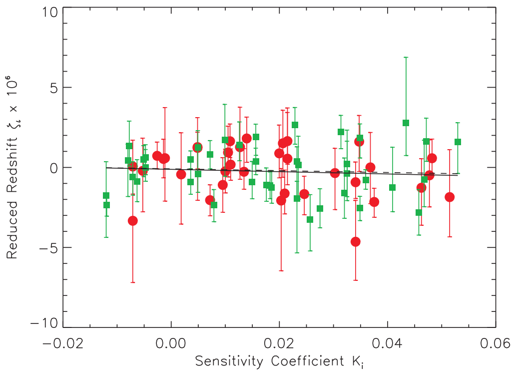


**Fig. 3.** The combined data plot of the reduced redshift $\zeta$ versus the sensitivity parameter K. The red dots are for Q0347-383 and the green squares are for Q0405-443. The error bars are $1\sigma$. The dashed line is the unweighted fit to the data, $\Delta\mu/\mu = -6 \times 10^{-6} \pm 10. \times 10^{-6}$ and the solid line the weighted fit to the data, $\Delta\mu/\mu = -7 \times 10^{-6} \pm 8 \times 10^{-6}$

### *5.1. Wavelength calibration*

An advantage of using $H_2$ for $\mu$ measurements is that each line has a unique sensitivity constant and therefore a unique shift which can not be mimiced by an error in redshift. In practice, however, the data quality is not good enough to match the particular pattern of shifts. We therefore try to compute a slope in the reduced redshift versus sensitivity factor plot. The sensitivity factors increase with increasing vibrational quantum number of the upper state. The lower state is always in the ground vibrational state. As the upper level vibrational quantum number increases the energy of the upper state increases and the wavelength of the transition decreases. This produces a correlation between wavelength and sensitivity factor with the sensitivity factor increasing as the wavelength decreases. A systematic error in the wavelength scale will then mimic a change in $\mu$. This is probably the source of the previously claimed positive detection of a change in $\mu$.

#### 5.1.1. Lyman and Werner line mix

One mitigation to the above systematic error possibility is the mixing of Lyman and Werner lines in the spectra. The higher electronic energy of the upper state of the Werner series produces shorter wavelength transitions with low vibrational quantum number and hence lower sensitivity factors at the same wavelengths as the high sensitivity lines of the Lyman series as shown in Figure 1. Mixtures of high sensitivity and low sensitivity lines can occur over short wavelength intervals where systematic wavelength calibration errors have a much smaller affect. A particular wavelength interval for Q0347-383 is shown in Figure 4.

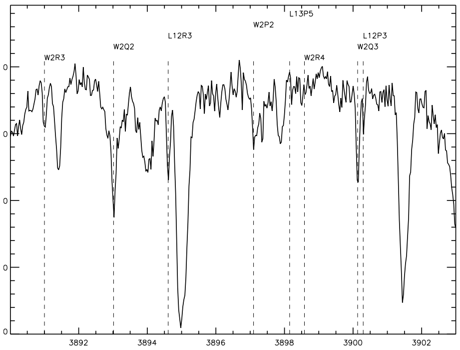


**Fig. 4.** A region of the spectrum of Q0347-383 that has a mixture of low sensitivity Werner (W) and high sensitivity Lyman lines (L). The number after the W or L designator is the vibrational quantum number of the upper state. Note that W2R3, L12R3, W2Q3 and L12P3 all have identical ground states.

In Thompson et al. (2009) the Werner lines were compared to their nearest Lyman lines in terms of wavelength and the histogram of the differences in redshift $\Delta z$ was plotted. For Q0405-443 there were an equal number of lines of positive and negative $\Delta z$ but for Q0347-383 all of the 7 $\Delta z$ values were negative. The figure from Thompson et al. (2009) is shown here as Figure 5. That all of the values are negative has a formal probability of $2^{-7} = 0.008$. Even though the probability is persuasive Thompson et al. (2009) refer to only a marginal possibility that a change in $\mu$ has been detected.

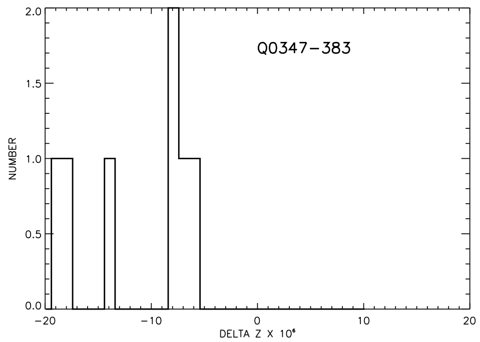


**Fig. 5.** Histogram of the delta redshift between each of the Werner band lines and their adjacent Lyman band lines for Q0347-383. A positive value means that the Lyman line had a higher redshift than the Werner line. Note that this is the delta redshift not the delta reduced redshift defined in Equation 3.

### *5.2. Errors in rest wavelengths of $H_2$*

Although the accuracy of the $H_2$ rest wavelengths from Ubachs et al. (2007) exceeds our current accuracy of astronomical measurements, improvement by a factor of 10 to 1 part in $10^6$ may require more accurate wavelength measurements. Typical sensitivity constants have values on the order of 0.02 and the typical wavelength errors are about a few time $10^{-8}$. Since the accuracy of measurements of $\Delta\mu/\mu$ scale as the wavelength error divided by the sensitivity factor, this leads to errors on the order of $10^{-6}$, which leaves no room in the error budget for other sources of error.

### *5.3. Errors in the sensitivity factor*

Errors in $\Delta\mu/\mu$ scale directly as errors in the sensitivity factors. If there is a systematic error in the sensitivity factors they will lead to the same order of error in $\Delta\mu/\mu$. A possibility is a systematic error in the sensitivity factor with increasing vibrational quantum number. This could lead to a false positive in the measurement. Since sensitivity factors are calculated from our knowledge of moleucular physics a systematic error in the approximations used in the calculation could produce a systematic sensitivity factor error

### *5.4. Instrumental errors*

In most spectrometers used to measure $\Delta\mu/\mu$ the light path of light from the observed object is not the same as the light path of the calibration lamp light. Differences in angle between the principal rays of the object and calibration light can introduce systematic wavelength differences even if the rest wavelengths of the calibration lines are accurately known. Similarly temporal instability on the time scale of the difference in time between object and calibration source observation can introduce errors.

## 6. Implications in particle physics and dark energy

In Grand Unified Theories (GUT) a rolling of $\mu$ is induced by time variations of the Quantum Chromodynamic (QCD) scale $\Lambda_{QCD}$ and the Higgs Vacuum Expectation Value (VEV) $\nu$. The relationship is generally expressed as

$$\frac{\dot{\mu}}{\mu} \approx \frac{\dot{\Lambda}_{QCD}}{\Lambda_{QCD}} - \frac{\dot{\nu}}{\nu} = R\frac{\dot{\alpha}}{\alpha} \tag{4}$$

where $\alpha$ is the fine structure and R is a scale factor. In many GUT theories R is large and negative ($R \approx -50$) (Avelino, Martins, Nunes & Olive 2006). If the claimed values for a change in $\alpha$ are substantiated the current constraints on changes in $\mu$ would be in conflict with such a high value of R.

Quintessence theories of Dark Energy are usually expressed in terms of a potential $V(\phi)$ that is a function of a rolling scalar $\phi$. In this formulation a change in $\mu$, $\Delta\mu$, would be a function of the scalar $\phi$ as given in equation 5 below.

$$\frac{\Delta\mu}{\mu} = \varsigma_\mu \kappa(\phi - \phi_0) \tag{5}$$

Here $\kappa$ is $\frac{\sqrt{8\pi}}{m_{Pl}}$, $m_{Pl}$ is the Planck mass and $\varsigma_\mu$ is a model dependent parameter. $\phi_0$ is the present day value of the scalar. A non-rolling or rolling value of $\mu$ can therefore act as a discriminator between a cosmological constant and quintessence as the proper origin of dark energy. The present day status of $\mu$ observations then define the regions of the landscape that are allowed by quintessence and the cosmological constant. The cosmological constant is confined to $\Delta\mu = 0$ while quintessence must live in the space defined in Figure 6.

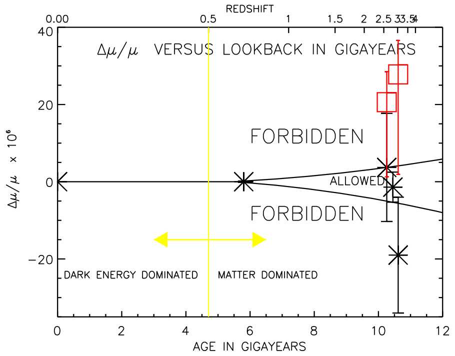


**Fig. 6.** This figure shows the current measurements of $\mu$ in the laboratory, by radio astronomy means and by optical observations of $H_2$. The outlying measurements in open boxes are the measurements from Reinhold et al. (2006) that were affected by wavelength errors. The measurements represented by asterisks are from King et al. (2009),Murphy et al. (2008) and Thompson et al. (2009). The boundary between dark energy dominated and matter dominated regions is marked with the arrows indicating the transition region.

## 7. Conclusions

From measurements made to date the value of $\mu$ is constant at the $\Delta\mu/\mu \leq 10^{-5}$ level for look back times up to 11 gigayears. This puts a legitimate constraint on high energy and cosmological physics. With larger telescopes and new instrumentation, improvement on this limit by a factor of 10 should be possible in the next 5 years. This will require strict attention to the sources of possible systematic errors. This makes the measurement of fundamental constants in the early universe a low cost and powerful tool for the study of cosmology and high energy physics.

*Acknowledgements.* The author is grateful for collaboration and engaging conversations with Jill Bechtold, John Black, Daniel Eisenstein, Xiaohui Fan, Rob Kennicutt, Carlos Martins, Xavier Prochaska, Yancy Shirley and Wim Ubachs.

## References

Avelino, P.P., et al. 2006, Phys. Rev. D,74, 083508
Cowie, L.L. & Songaila, A. 1995 ApJ, 453, 596
Cui, J., Bechtold, J., Ge, J. & Meyer, D.M. 2005, ApJ, 633, 649
Dirac, P.A.M. 1937, Nature, 139, 323
D'Odorico, S., Dessauges-Zavadsky, M., & Molaro, P. 2001, A&A, 368, L21
Flambaum, V.V. & Kozlov, M.G. 2007, Phys. Rev. Lett., 98, 240801
Foltz, C. B., Chaffee, F.H., & Black, J.H. 1988,
Gamow, G. 1967, Phys. Rev. Lett., 19, 759
King, J. A., et al. 2009, Phys. Rev. Lett., 101, 251304
Ivanchik, A.V. et al. 2002, Astronomy Letters, 28, 423 (page 483 in Asttronomicheskii Zhurnal)
Ivanchik, A., Petitjean, P., Rodriguez, E. & Varshalovich, et al.. 2003, Ap&SS, 283, 583
Ivanchik, A. et al. 2005, A&A, 440, 45
Levshakov, S. A. et al. 2002, MNRAS, 333, 373.
Levshakov, S. A., Molaro, P. & Kozlov, M. G. 2008 `astro-ph0808.0583v1`
Murphy, M.T., et al. 2008, Science, 320, 1611
Potekhin, A.Y. et al. 1998, ApJ, 505, 523
Reinhold, E. et al. 2006, Phys. Rev. Lett., 96, 151101
Teller, E. 1948, Phys. Rev., 73, 801
Thompson, R.I. 1975 Astrophysical Letters, 16, 3
Thompson, R.I. et al. 2009 ApJ, 703, 1648.
Ubachs, W. & Reinhold 2004, Phys. Rev. Lett., 92, 101302
Ubachs, W., et al. 2007, Jour. Mol. Spec., 241, 155
Varshalovich, D. & Levshakov, S. 1993, JETP Letters, 58, 231
Wendt, M. & Reimers, D. 2008, Eur. Phys. J. ST, 163, 197